Aeronautical Research Institute, University of Tokyo
Report No. 347, July 1959

The Stress Distribution in a Swept-back Box-beam under Torsional and Bending Loads*

By

Ken IKEDA and Megumi SUNAKAWA

Summary An approximate solution is presented to obtain the static stress distributions in a swept-back box-beam having asymmetrical section. The box-beam is assumed to consist of four concentrated flanges of different cross-sectional area and four thin walls of different thickness, which connect the flanges. The ribs are assumed perfectly stiff except the one nearest to the root.

1. GENERAL

1.1. *Introduction*

We present an approximate method for the stress analysis of swept-back wing structures.

Hitherto, the wing structure has been reduced to a box-beam for the convenience of analysis. After World War II the performance of airplane has progressed very quickly, and most of them fit swept-back wings. In these cases, too, the wings have been frequently analyzed as box-beams by many investigators. For example, Dr. Levy [*1*] solved the problems using "influence coefficients". However, the calculation seemed rather difficult and tedious.

In this paper, we have analyzed the stress distribution in wing structures on the basis of the general method for the statically indeterminate structural analysis. The method for the statically indeterminate structural analysis was proposed by H. Reissner [*2*] originally. The key-point of applying this method to the structural analysis is how to construct the equilibrating systems in the object.

The fundamental principle of this method is the theory of least work and even complex statically indeterminate structures can be analyzed easily by constructing the equilibrating systems.

In this analysis, the ribs parallel to air stream are replaced by the ones perpendicular to the spars. And it was ascertained by Lang and Bisplinghoff [*3*] that this replacement had little effect on the strength of box-beam and the processes of analysis were greatly simplified by such a replacement.

1.2. *Symbols and abbreviations*

a, b depth and width of the cross-section of box-beam (Fig. 2).

* Presented at the Annual Meeting of the Japan Society of Aeronautical Engineering, April 11, 1958.

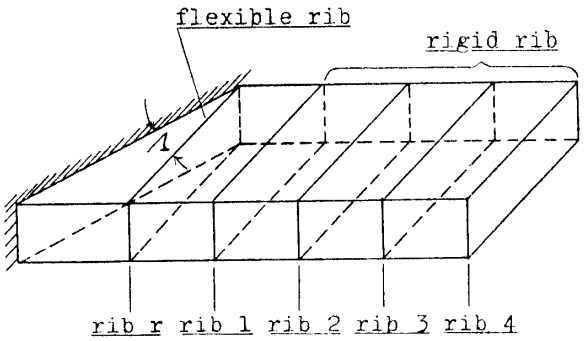

FIGURE 1. Schematic drawing of box-beam.

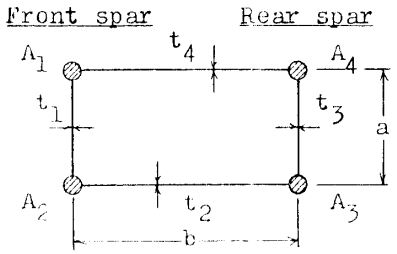

FIGURE 2. Cross-section of box-beam.

d_i distance between $(i-1)$th and i-th ribs.
d_r distance between the root and the first rib r in the front spar.
q shear flow.
$t_{1i}, \cdots, t_{4i}$ thicknesses of webs at the i-th bulkhead (Fig. 2).
t_{Ri} thickness of the i-th rib.
$A_{1i}, \cdots, A_{4i}$ cross-sectional areas of flanges at the i-th bulkhead (Fig. 2).
E Young's modulus.
G modulus of shear rigidity.
P axial force in flange.
Q vertical load.
T torsional load.
X statically indeterminate quantity in the equilibrating system.
Λ angle of sweep.

$$\alpha' = -\frac{a}{t_{1r}} + \left(\frac{b}{t_{2r}} + \frac{b}{t_{4r}}\right) \times \frac{1}{2} .$$

$$\alpha_1 = \frac{a}{t_{1r}} + \left(\frac{b}{t_{2r}} + \frac{b}{t_{4r}}\right) \times \frac{1}{2} .$$

$$\alpha_{2i} = \frac{1}{A_{1i}} + \frac{1}{A_{2i}} .$$

$$\alpha'_{2i} = \frac{1}{A_{3i}} + \frac{1}{A_{4i}} .$$

$$S'_i = -\frac{a}{t_{1i}} + \frac{b}{t_{2i}} - \frac{a}{t_{3i}} + \frac{b}{t_{4i}} .$$

$$S_{1i} = \frac{a}{t_{1i}} + \frac{b}{t_{2i}} + \frac{a}{t_{3i}} + \frac{b}{t_{4i}} .$$

$$S_{2i} = \frac{1}{A_{1i}} + \frac{1}{A_{2i}} + \frac{1}{A_{3i}} + \frac{1}{A_{4i}} .$$

$$m_i = \frac{d_r}{d_i} .$$

$$\gamma = \frac{ab}{d_r t_{Rr}} .$$

Subscripts:

"0" denotes the amount referring to principal system.

r and $1, 2, \cdots, j, k, \cdots$ denote amounts referring to self-equilibrating systems at root and other places.

2. The Method of Analysis

2.1. *Systems of stresses*

As described above, the construction of equilibrating systems is the kernel of this analysis. We accomplished the analysis successfully by using the following systems.

2.1.1. *The principal system*

The principal systems are taken so as to equilibrate the external forces and the primary stresses of the structure for each case.

2.1.2. *The self-equilibrating systems*

In the analysis of a swept-back box-beam, we construct the self-equilibrating systems at the root and at each rib station except the tip one as shown in Fig. 3.

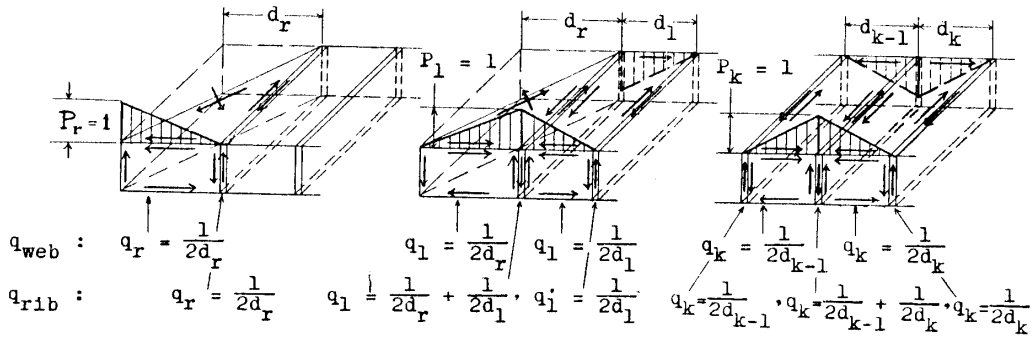

FIGURE 3. Self-equilibrating system.

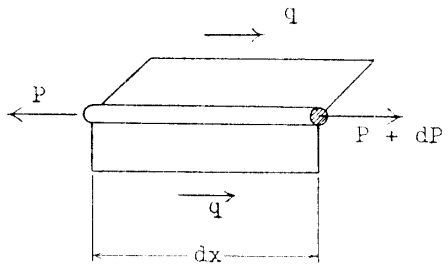

FIGURE 4. Relation between flange force and shear flow.

From the equilibrium condition between flange force and shear flow (Fig. 4), the following equation can be obtained:

$$\frac{dP}{dx} = -2q\,.$$

Using the boundary conditions,

$$P=0 \quad \text{at} \quad x=l \quad \text{and} \quad P=1 \quad \text{at} \quad x=0$$

on a flange force in each of self-equilibrating systems, then, the shear flow is given by

$$q = \frac{1}{2l} .$$

2.2. *Elasticity equations*

On the swept-back box-beam with $n+1$ ribs, the elasticity equations can be summarized as follows:

$$\begin{pmatrix} \delta_{rr} & \delta_{1r} & \cdots & \delta_{nr} \\ \delta_{r1} & \delta_{11} & \cdots & \delta_{n1} \\ \cdot & \cdot & \cdots & \cdot \\ \cdot & \cdot & \cdots & \cdot \\ \delta_{rn} & \delta_{1n} & \cdots & \delta_{nn} \end{pmatrix} \begin{pmatrix} X_r \\ X_1 \\ \cdot \\ \cdot \\ X_n \end{pmatrix} = - \begin{pmatrix} \delta_{0r} \\ \delta_{01} \\ \cdot \\ \cdot \\ \delta_{0n} \end{pmatrix}, \tag{2.2-1}$$

where

$$\left.\begin{aligned}
\delta_{0k} &= \sum_{(k-1)\,\text{web}} \int \frac{q_0 q_k}{Gt} dF + \sum_{(k)\,\text{web}} \int \frac{q_0 q_k}{Gt} dF \\
&\quad + \sum_{(k-1)\,\text{flange}} \int \frac{P_0 P_k}{EA} dx + \sum_{(k)\,\text{flange}} \int \frac{P_0 P_k}{EA} dx , \\
\delta_{kk} &= \sum_{(k-1)\,\text{web}} \int \frac{q_k^2}{Gt} dF + \sum_{(k)\,\text{web}} \int \frac{q_k^2}{Gt} dF \\
&\quad + \sum_{(k-1)\,\text{flange}} \int \frac{P_k^2}{EA} dx + \sum_{(k)\,\text{flange}} \int \frac{P_k^2}{EA} dx \\
&\quad + \int_{(k-1)\,\text{rib}} \frac{q_k^2}{Gt_{R(k-1)}} dF + \int_{(k)\,\text{rib}} \frac{q_k^2}{Gt_{Rk}} dF + \int_{(k+1)\,\text{rib}} \frac{q_k^2}{Gt_{R(k+1)}} dF , \\
\delta_{(k+1)k} &= \sum_{(k)\,\text{web}} \int \frac{q_{k+1} q_k}{Gt} dF + \sum_{(k)\,\text{flange}} \int \frac{P_{k+1} P_k}{EA} dx \\
&\quad + \int_{(k)\,\text{rib}} \frac{q_{k+1} q_k}{Gt_{Rk}} dF + \int_{(k+1)\,\text{rib}} \frac{q_{k+1} q_k}{Gt_{R(k+1)}} dF , \\
\delta_{(k+2)k} &= \int_{(k+1)\,\text{rib}} \frac{q_{k+2} q_k}{Gt_{R(k+1)}} dF , \\
(\delta_{jk})_{(j-k)>2} &= 0 .
\end{aligned}\right\} \tag{2.2-2}$$

By solving the elasticity equations (2.2-1), we can obtain flange forces and shear flows in webs in a swept-back box-beam.

2.3. *Flange force*

By using Xs solved from the elasticity equations (2.2-1), the flange force P_K between $(k-1)$th and k-th ribs is represented as Eq. (2.2-3), taking the position of $(k-1)$th rib as the origin of coordinates.

$$P_K = P_0 + X_k\left(1 - \frac{x}{d_k}\right) + X_{k+1}\left(\frac{x}{d_k}\right). \tag{2.2-3}$$

2.4. *Shear flow in web*

The shear flow q_K between $(k-1)$th and k-th ribs is represented as follows:

$$q_K = q_0 + q_k X_k - q_{k+1} X_{k+1} . \tag{2.2-4}$$

3. Examples of Application of the Method

We present how to apply this method to practical cases on a swept-back box-beam under tip concentrated torsional or bending load for a typical case.

3.1. *Basic assumptions*

To simplify the problems we introduce the following assumptions.

(1) Wing is a monocoque structure having two spars and has a rectangular cross-section, which is composed of four concentrated flanges and four webs connecting the formers. Taper is not taken into consideration.
(2) Attachments of wing to the fuselage are perfectly rigid.
(3) Bulkheads have infinitely large stiffness in their own planes. Each section, therefore, keeps the shape of the initial rectangular cross-section after loading, but is perfectly flexible for the deflection normal to its plane.
(4) Webs and ribs have the rigidity only against the shear force in their own planes, and have no stiffness for the rotation and bending of their planes.
(5) Young's modulus E of flanges and modulus of shear rigidity G of webs are constant and independent of values of stresses.
(6) All components do not buckle.
(7) Wing is composed of five ribs. Flexibilities of ribs are not considered except for the root one. (Fig. 1)

3.2. *Analysis of the case under a tip concentrated torsional load*

In the webs of box-beam under torsional load, shear flows are not constant as given by the formula of Bredt or Batho, but secondary stresses are set up by the resulting interference effect, if axial constraints exist.

Now, in the swept-back box-beam with five ribs under torsional load (Fig. 5), we take the principal system as shown in Fig. 6 and the self-equilibrating systems as shown in Fig. 3, respectively. Shear flows in the root delta webs are assumed

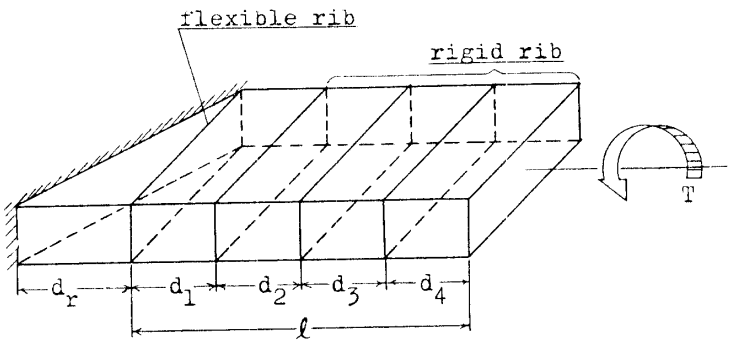

FIGURE 5. Box-beam under a tip concentrated torque.

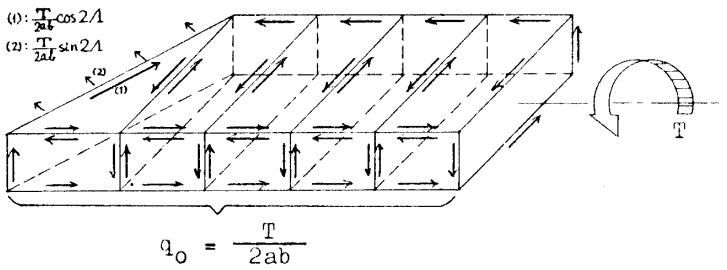

FIGURE 6. Principal system (Torsional load).

to be uniform also and all ribs except the rib r are perfectly rigid. In the principal system, we put the shear flow q_{0k} as $q_{0k}=T/2ab$.

The elasticity equations are obtained putting $n=4$ in Eqs. (2.2–1) and δs of Eqs. (2.2–2) are calculated as follows:

$$\delta_{0r}=-\frac{1}{2G}\alpha'\frac{T}{2ab},$$

$$\delta_{rr}=\frac{1}{4Gd_1}\frac{(\alpha_1+\gamma)}{m_1}+\frac{d_1}{3E}m_1\alpha_{2r},$$

$$\delta_{1r}=-\frac{1}{4Gd_1}\left\{\frac{\alpha_1+\gamma(1+m_1)}{m_1}\right\}+\frac{d_1}{6E}m_1\alpha_{2r},$$

$$\delta_{2r}=\frac{1}{4Gd_1}\gamma,$$

$$\delta_{01}=-\frac{1}{2G}(S_1'-\alpha')\frac{T}{2ab},$$

$$\delta_{11}=\frac{1}{4Gd_1}\left\{S_{11}+\frac{\alpha_1+\gamma(1+m_1)^2}{m_1}\right\}+\frac{d_1}{3E}(S_{21}+m_1\alpha_{2r}),$$

$$\delta_{21}=-\frac{1}{4Gd_1}\{S_{11}+\gamma(1+m_1)\}+\frac{d_1}{6E}S_{21},$$

$$\delta_{22}=\frac{1}{4G}\left\{\left(\frac{S_{11}}{d_1}+\frac{S_{12}}{d_2}\right)+\frac{m_1\gamma}{d_1}\right\}+\frac{1}{3E}(d_1S_{21}+d_2S_{22}),$$

$$(\delta_{0k})_{k=2,3,4}=-\frac{1}{2G}(S_k'-S_{k-1}')\frac{T}{2ab},$$

$$(\delta_{kk})_{k=3,4}=\frac{1}{4G}\left(\frac{S_{1(k-1)}}{d_{k-1}}+\frac{S_{1k}}{d_k}\right)+\frac{1}{3E}(d_{k-1}S_{2(k-1)}+d_kS_{2k}),$$

$$(\delta_{(k+1)k})_{k=2,3}=-\frac{1}{4Gd_k}S_{1k}+\frac{d_k}{6E}S_{2k},$$

$$(\delta_{jk})_{(j-k)\geq 2}=0.$$

3.3. *Analysis of the case under a bending moment due to tip load*

When a vertical load Q is applied to the tip of front spar of the two-spar wing construction, for example, the front spar deflection is constrained by its own bending rigidity and by the torsional rigidity of the wing as a whole. In consequence, a part of loads transfers to the rear spar through shear flows at every rib station.

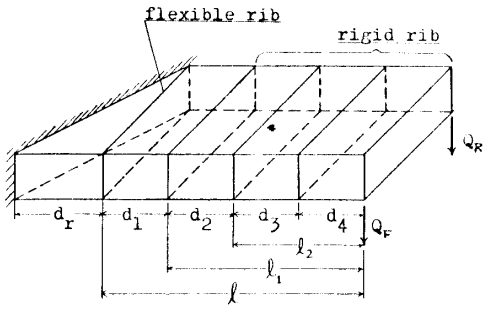

FIGURE 7. Box-beam under a tip concentrated bending load.

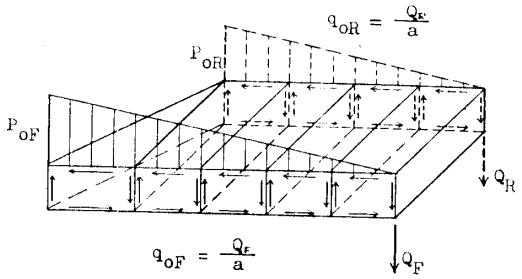

FIGURE 8. Principal system (Bending load).

Now, in the swept-back box-beam with five ribs under bending load (Fig. 7), we take the principal system under a tip load on the front or rear spar separately as shown in Fig. 8, and the self-equilibrating systems are the same as shown in Fig. 3–a, b, c. Shear flows in all panels are uniform, and all ribs except the rib r are perfectly rigid. In the principal system, shear flow Q/a exists in a spar web.

(a) *The case when a tip load is applied only on the front spar*

The elasticity equations are obtained putting $n=4$ in Eqs. (2.2–1), where

$$\delta_{0r}=\left\{\frac{1}{2G}\frac{a}{t_{1r}}+\frac{\alpha_{2r}}{E}\left(\frac{ld_r}{2}+\frac{d_r^2}{3}\right)\right\}\frac{Q_F}{a},$$

$$(\delta_{0k})_{k=1,2,3,4}=\left[\frac{1}{2G}\left(\frac{a}{t_{1k}}-\frac{a}{t_{1(k-1)}}\right)+\frac{\alpha_{2k}}{2E}\left\{(l_kd_k+l_{k-1}d_{k-1})+\frac{1}{3}(2d_k^2+d_{k-1}^2)\right\}\right]\frac{Q_F}{a}.$$

Other δs are the same as those described in section 3.2.

(b) *The case when a tip load is applied only on the rear spar*

The elasticity equations are obtained putting $n=4$ in Eqs. (2.2–1), where

$$\delta_{0r}=0,$$

$$\delta_{01}=\left\{\frac{1}{2G}\frac{a}{t_{11}}+\frac{\alpha'_{21}}{E}\left(\frac{l_1d_1}{2}+\frac{d_1^2}{3}\right)\right\}\frac{Q_R}{a}.$$

Other δs are the same as those in the case of (a) except that Q_R and α'_{2i} must be replaced by Q_F and α_{2i}.

3.4. *Numerical examples*

3.4.1. *Dimensions of the model used for a numerical example*

$l=1000\,\text{mm}$, $a=150\,\text{mm}$, $b=300\,\text{mm}$, $d_1=d_2=d_3=d_4=250\,\text{mm}$,
$d_r=b\tan\Lambda=300\tan\Lambda$, $(\Lambda=0°, 15°, 30°, 45°, 60°)$,
$t_{1i}=t_{3i}=1.5\,\text{mm}$, $t_{2i}=t_{4i}=1.0\,\text{mm}$, $t_{Ri}=1.2\,\text{mm}$,
$A_{1i}=A_{2i}=A_{3i}=A_{4i}=500\,\text{mm}^2$, $E=7000\,\text{kg/mm}^2$, $G=2750\,\text{kg/mm}^2$.

TABLE 1. X_is in a torsional load

X_i \ Λ	0°	15°	30°	45°	60°
$X_r/(T/b)$	—	0.88	0.92	0.89	0.75
$X_1/(T/b)$	0.81	0.70	0.58	0.44	0.30
$X_2/(T/b)$	0.29	0.24	0.19	0.15	0.10
$X_3/(T/b)$	0.10	0.08	0.07	0.05	0.04
$X_4/(T/b)$	0.03	0.03	0.02	0.02	0.01

3.4.2. *Numerical results and remarks*

Numerical results are summarized in Fig. 9~Fig. 14, inclusive.

3.4.2.1. *Results of the case under a tip concentrated torsional load (Figs. 9, 10 and 11)*

The calculated values of X_is are shown in Table 1. The distributions of axial forces in flanges for various angles of sweep-back are plotted in Fig. 9 and the variations of flange force and shear flow at the root with the angle of sweep-back are shown in Fig. 10 and Fig. 11, respectively. We can see that the flange forces at the root decrease considerably with the increase of the angles of sweep-back. For example, the axial flange force at the root in the case of $\Lambda=45°$ reduces to

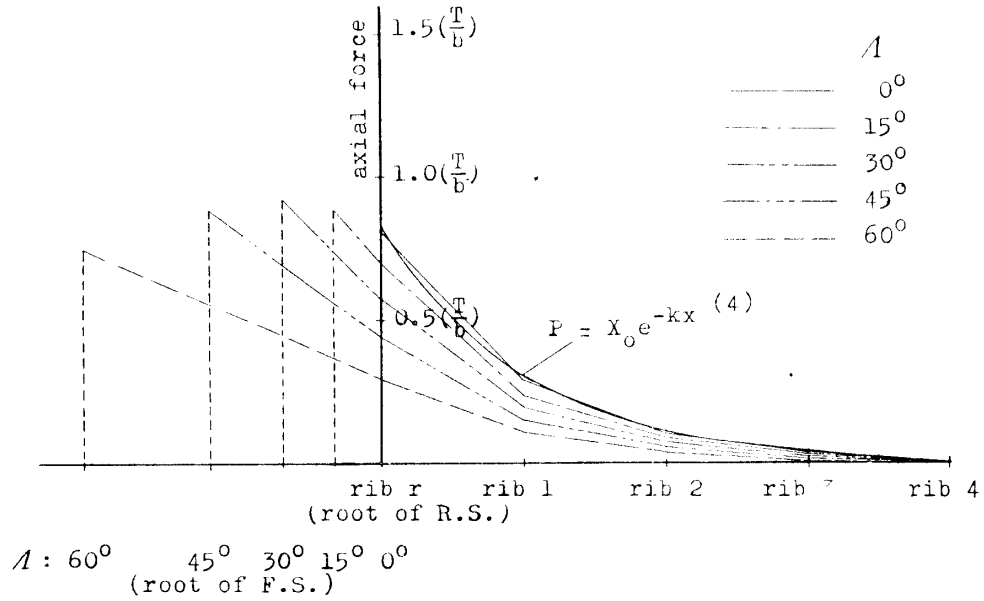

FIGURE 9. Axial forces in flanges due to a tip concentrated torsional load.

about 50% of that of $\Lambda=0°$. On the other hand, when $\Lambda=0°$ the shear flow in the spar web at the root increases about 30% compared with those given by the formula of Bredt or Batho. And, the influence of sweep-angle on shear flows is not so remarkable.

We added the curve of flange force in Fig. 9, which was obtained by one of the authors [4] for a box-beam with closely spaced ribs when $\Lambda=0°$. A satisfactory agreement with the results can be seen in this paper.

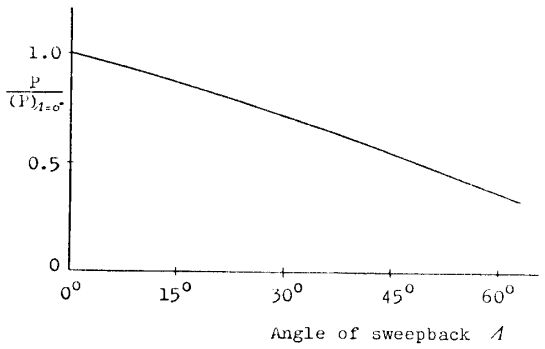

FIGURE 10. Axial force in flange at root due to a torsional load.

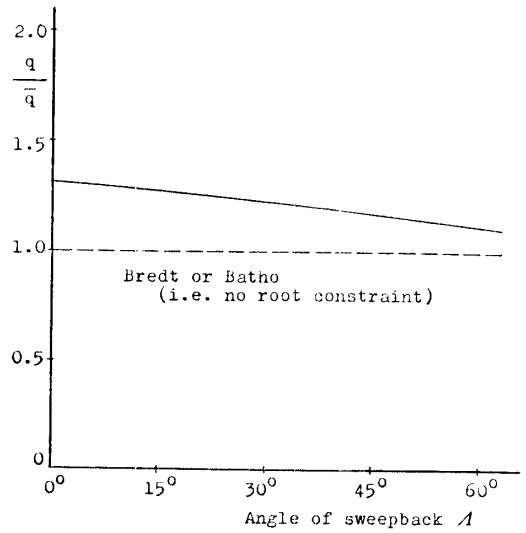

FIGURE 11. Shear flow in spar web at root due to a torsional load.

3.4.2.2. *Results of the case under tip bending loads on two spars (Figs. 12, 13 and 14)*

The calculated values of X_is are shown in Table 2. The case, where two bending loads are equal ($Q_F=Q_R=Q$), is considered. In this case, the flange forces and the shear flows vary very much with sweep angles. For example, the flange force and the spar web shear flow at the rear spar root in the case of $\Lambda=45°$ increases about 35% and about 45%, respectively, compared with those in the case of $\Lambda=0°$, and the variation of shear flows with angles of sweep-back is larger than that of flange forces. The corresponding decreases occur in the front spar.

TABLE 2. X_is in a bending load

Λ	0°	15°	30°	45°	60°
X_{rF}/Q	—	−3.82	−5.00	−6.61	−9.08
X_{rR}/Q	—	2.50	1.90	1.17	0.30
X_{1F}/Q	−2.93	−3.46	−3.90	−4.26	−4.56
X_{1R}/Q	2.93	2.51	2.20	1.97	1.82
X_{2F}/Q	−2.36	−2.51	−2.67	−2.79	−2.89
X_{2R}/Q	2.36	2.21	2.14	2.06	2.01
X_{3F}/Q	−1.62	−1.66	−1.73	−1.77	−1.80
X_{3R}/Q	1.62	1.55	1.54	1.51	1.49
X_{4F}/Q	−0.82	−0.82	−0.85	−0.86	−0.88
X_{4R}/Q	0.82	0.79	0.79	0.78	0.78

Suffix $F(R)$ denotes that the load is applied on the front (rear) spar.

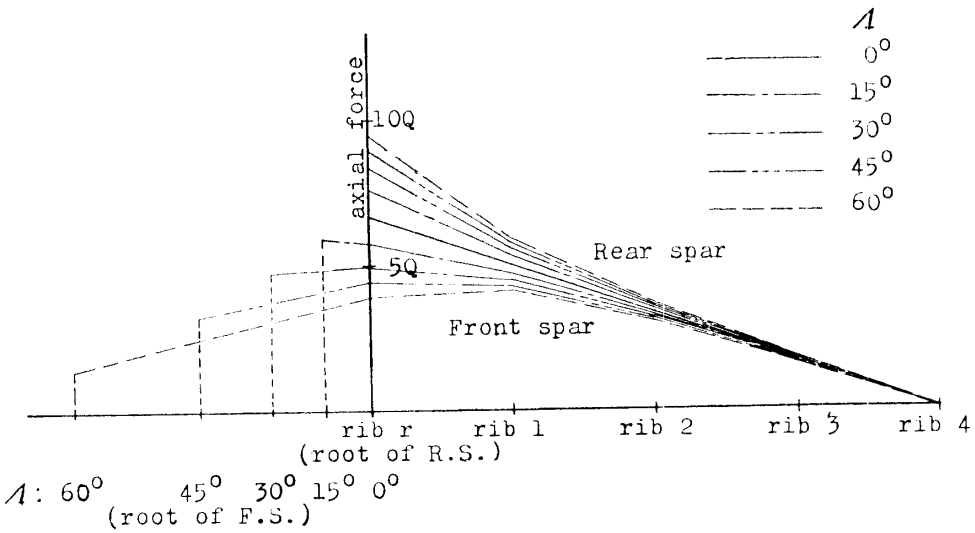

FIGURE 12. Axial forces in flanges due to a tip concentrated bending load.

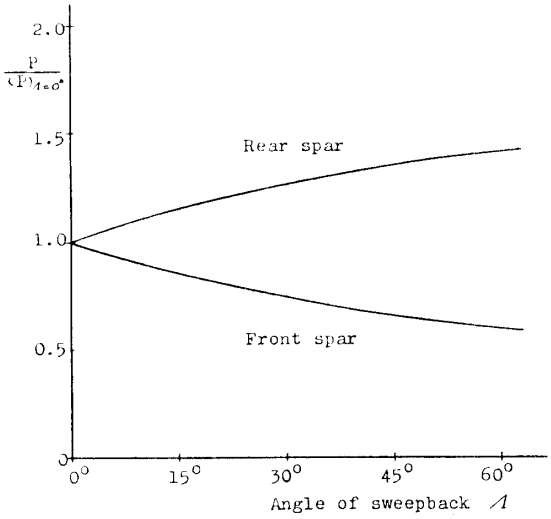

FIGURE 13. Axial force in flange at root due to a bending load.

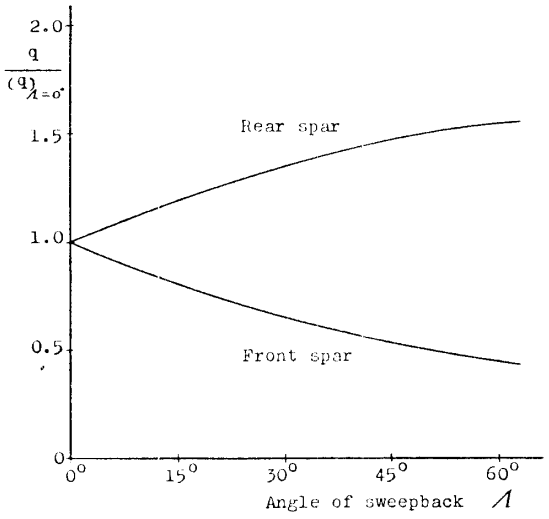

FIGURE 14. Shear flow in spar web at root due to a bending load.

4. CONCLUSIONS

We presented an approximate method for calculating the stress distributions in a swept-back box-beam. It seems that this method has a good accuracy in spite of using some assumptions and simplifications in the examples of application.

In the examples of application, we neglected the flexibilities of all ribs except the root one. But, since even the effect of flexibility of the root rib is not so large in our calculation and so the effect of the other ribs may be very smaller, this neglect seems practical and contributes greatly to the simplification of calculation. Some practical wings have more ribs than five, but in the analysis, we suggest to replace their ribs by five ribs; the root one as it is and four ribs having infinite shear stiffness.

Moreover, we assumed that the buckling of components does not occur, but in the condition of tension field, for example, the use of equivalent modulus of shear rigidity G_e seems to widen the field of application of this method.

Department of Structures,
Aeronautical Research Institute,
University of Tokyo, Tokyo.
February 11, 1958.

References

[*1*] Williams, M. L.: A Review of Certain Analysis Method for Swept Wing Structure, J. A. S., Vol. 19, No. 9, (1952/9), p. 615.
Levy, S.: Computation of Influence Coefficients for Aircraft Structures with Discontinuities, J.A.S., Vol. 14, No. 10, (1947/10), p. 547.

[*2*] Reissner, H.: Neuere Probleme aus der Flugzeugstatik, Z.F.M, 17 Jahrg., 18 Heft, (1926), S. 384.
Ebner, H.: Die Beanspruchung duennwandiger Kastentraeger auf Drillung bei behinderter Querschnittswoelbung, Z.F.M., 24 Jahrg., Nr. 23, S. 645 u. S. 684, (1933/12).

[*3*] Lang, A. L. and Bisplinghoff, R. L.: Some Results of Sweptback Wing Structural Studies, J.A.S., Vol. 18, No. 11, (1951/11), p. 705.

[*4*] Ikeda, K.: Approximate Analysis of Swept-Wing Structure, J. Japan Soc. Aero. Engg., Vol. 1, No. 3, (1953/10), p. 132.